Physical Layer Security Performance of Wireless Mobile Sensor Networks in Smart City

HAN WANG[1], (Member, IEEE), **LINGWEI XU**[2,3], (Member, IEEE), **WENZHONG LIN**[3],
PINGPING XIAO[1], **AND RUHONG WEN**[1]

[1]College of Physical Science and Engineering, Yichun University, Yichun 336000, Jiangxi, China
[2]School of Information Science and Technology, Qingdao University of Science and Technology, Qingdao 266061, Shandong, China
[3]Fujian Provincial Key Laboratory of Information Processing and Intelligent Control, Minjiang University, Fuzhou 350121, Fujian, China

Corresponding authors: Han Wang (hanwang1214@126.com) and Lingwei Xu (gaomilaojia2009@163.com)

ABSTRACT In smart cities, the ubiquitous network connections and high data rate services are provided to afford effective service of real-time monitoring and responses. With the development of the 5G mobile communication technology, the wireless sensor mobile communication networks in the smart city have become a hot issue for academic researches. Due to the openness of wireless channels, the physical layer security of the wireless mobile sensor mobile communication networks in smart city encounters severe challenges. In this paper, based on Wyner's wiretap model, the secrecy performance of the wireless mobile sensor communication networks over 2-Nakagami fading channels is investigated. We derive the exact secure outage probability (SOP) and the probability of strictly positive secrecy capacity expressions for two transmit antenna selection (TAS) schemes. The exact closed-form expressions for the lower bound on the SOP are also derived using the optimal TAS scheme. Then, the system secrecy performance is verified and analyzed by Monte Carlo simulations under different conditions. The simulation results show that the analytical results match perfectly with the Monte Carlo simulation results. Increasing the number of transmit antennas can improve secrecy performance.

INDEX TERMS Smart city, wireless mobile sensor networks, physical layer security, secure outage probability, probability of strictly positive secrecy capacity, transmit antenna selection.

I. INTRODUCTION

In recent years, the academic and industrial fields have paid close attention to the smart city [1]–[3]. The smart city has various applications, such as smart healthcare, smart transportation, and smart homes [4]. The mobile communication plays an important role to achieve these smart applications via massive deployment of physical objects, such as sensors, controllers, and actuators [5]–[8]. So the wireless sensor network has been seen as an important engine for the growth and progress of smart city.

Due to the openness of mobile channels, the mobility of terminals and the diversity of network architectures,

the physical layer security of wireless sensor network is facing a severe challenge. And it has become a hot topic in the 5G mobile communication technology. Researchers have studied the safety technology of physical layer in various aspects [9]–[11]. In [12], in the presence of an eavesdropper, the transmission of confidential messages in a single-input multiple-output (SIMO) system is investigated.

For the wireless sensor network in smart city, multiple antenna technology is an effective approach to improve the secrecy performance. In [13], in the presence of an eavesdropper, the authors consider the problem of secret communication and derive the close-form expressions for the secrecy outage probability (SOP). In [14], employing transmit antenna selection (TAS) scheme, the authors analyze the physical layer security. The closed-form expressions for SOP

The associate editor coordinating the review of this manuscript and approving it for publication was Liangtian Wan.

and the low bound on average secrecy capacity (ASC) are derived, respectively. Then, the physical layer security of multiple antenna system using TAS has been analyzed in [15]. What's more, to enhance physical layer security, the authors analyze the probability of strictly positive secrecy capacity (SPSC) using TAS over Nakagmi-m channels in [16]. Cao *et al.* [17] propose two schemes to improve the sum rate of secondary users (SUs) and guarantee the secrecy rate of primary user (PU). A novel hybrid scheme for the lower complexity of beam-forming scheme and higher security of TAS is also proposed in [18]. Based on the channel phase, a physical-layer security scheme is proposed to secure the transmitted data [19]. References [20]–[23] investigate the malicious attacks in target detection wireless sensor networks (WSNs). The physical layer security performance of the mobile vehicular networks is investigated in [24].

However, the existing researches on the physical layer secrecy performance are mainly based on the Rayleigh and Nakagmi channels. The existing studies do not cover the mobile communication channel model in the actual environment. Experimental and theoretical analysis shows that Rayleigh and Nakagami channel models can not exactly describe the dynamic characteristics of mobile communication channels [25], [26]. The 2-Rayleigh and 2-Nakagami fading models have been considered for mobile communication channels in [27]–[30]. The 2-Nakagami channels can flexibly characterize the fading characteristics of wireless mobile channels, so it is more widely applicable and complex than 2-Rayleigh, Rayleigh and Nakagmi channels.

To the best of our knowledge, the physical layer security of mobile wireless sensor networks in smart city has not been considered in the literature. In this paper, the physical layer secrecy performance of mobile wireless sensor networks in smart city over 2-Nakagami channel is investigated. We present the quantitative analysis of physical layer secrecy performance with SOP and probability of SPSC as indicators. The optimal and suboptimal transmit antenna selection (TAS) schemes are proposed in this paper. For the two TAS schemes, we derive the exact closed-form SOP and probability of SPSC expressions, respectively. We also derive the exact closed-form expressions for the lower bound on the SOP using the optimal TAS scheme. Then, the system secrecy performance is verified and analyzed by Monte-Carlo simulation under different conditions.

The rest of this paper is organized as follow. In Section II, the system model is described. The SOP and probability of SPSC performance of the two TAS schemes is investigated in Section III and Section IV. Section V presents the Monte-Carlo simulation results. Finally, we conclude the paper in Section VI.

II. SYSTEM MODEL

Fig. 1 shows the multiple antenna wireless sensor networks model in smart city. Based on Wyner's wiretap model, the system includes a mobile source (S) sensor, a mobile legal destination (D) sensor and a mobile eavesdropper (E) sensor.
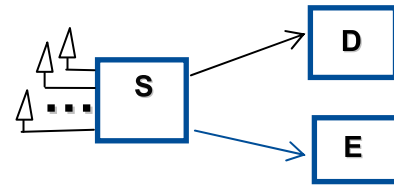

FIGURE 1. Multiple antenna wireless sensor communication networks model.

S sends information to D. E can obtain the information via the eavesdropping channel. The S is equipped with Nt antennas, the D and E are equipped with single antenna.

In the following, h denotes the channel coefficient, which follows the 2-Nakagami distribution [25]

$$h = \prod_{l=1}^{2} a_l \qquad (1)$$

where a_l is a Nakagami distributed random variable. The probability density function is given as

$$f(a) = \frac{2m^m}{\Omega^m \Gamma(m)} a^{2m-1} \exp(-\frac{m}{\Omega} a^2) \qquad (2)$$

where m is the fading coefficient, $\Omega = E(|a|^2)$ is a scaling factor, $E[\cdot]$ denotes the mean value, and $\Gamma(\cdot)$ is the Gamma function.

The probability density function of h is given by [25]

$$f(h) = \frac{2}{h \prod_{t=1}^{N} \Gamma(m_t)} G_{0,2}^{2,0} \left[h^2 \prod_{t=1}^{2} \frac{m_t}{\Omega_t} \Big|_{m_1, m_2}^{-} \right] \qquad (3)$$

where G[·] is the Meijer's G-function.

V_{SD} is the relative gain of the S to D link, and V_{SE} is the relative gain of the S to E link. D and E receive the signals as

$$r_{SDi} = \sqrt{V_{SD}E} h_{SDi} x + n_{SDi} \qquad (4)$$

$$r_{SEi} = \sqrt{V_{SE}E} h_{SEi} x + n_{SEi} \qquad (5)$$

where x is transmitted signal, which has mean 0 and variance 1, n_{SDi} and n_{SEi} are additive white Gaussian noise (AWGN), which has mean 0 and variance $N_0/2$, and E is the emission power of x.

The corresponding received SNR at D is given as

$$\gamma_{SDi} = \frac{K V_{SD} |h_{SDi}|^2 E}{N_0} \qquad (6)$$

The average received SNR is given as

$$\overline{\gamma_{SD}} = K V_{SD} \overline{\gamma} \qquad (7)$$

$$\overline{\gamma} = \frac{E}{N_0} \qquad (8)$$

where K is the SNR gain of the main channel relative to the eavesdropping channel.

The corresponding received SNR at E is given as

$$\gamma_{SEi} = V_{SE} |h_{SEi}|^2 \overline{\gamma} \qquad (9)$$

The average received SNR at E is given as

$$\overline{\gamma_{SE}} = V_{SE}\overline{\gamma} \tag{10}$$

The cumulative distribution function of γ_k, $k \in \{SD,SE\}$, is given as

$$F_{\gamma_k}(r) = \frac{1}{\prod\limits_{i=1}^{N} \Gamma(m_i)} G_{1,3}^{2,1}\left[\frac{r}{\overline{\gamma_k}} \prod_{i=1}^{2} \frac{m_i}{\Omega_i} \Big|_{m_1,.m_2,0}^{1}\right] \tag{11}$$

The probability density function of γ_k is given as

$$f_{\gamma_k}(r) = \frac{1}{r \prod\limits_{i=1}^{N} \Gamma(m_i)} G_{0,2}^{2,0}\left[\frac{r}{\overline{\gamma_k}} \prod_{i=1}^{2} \frac{m_i}{\Omega_i} \Big|_{m_1,m_2}^{-}\right] \tag{12}$$

Instantaneous security capacity is defined as [31]

$$C_i = \max \{\ln(1 + \gamma_{SDi}) - \ln(1 + \gamma_{SEi}), 0\} \tag{13}$$

For the optimal TAS scheme, we select the transmit antenna w as

$$w = \max_{1 \le i \le N_t} (C_i) \tag{14}$$

For the suboptimal TAS scheme, we select the transmit antenna g as

$$g = \max_{1 \le i \le N_t} (\gamma_{SDi}) \tag{15}$$

III. THE SOP OF THE OPTIMAL AND SUBOPTIMAL TAS SCHEME

We obtain the SOP of the optimal TAS scheme as

$$
\begin{aligned}
F_{\text{optimal}} &= \Pr(\max_{1 \le i \le N_t} (C_i) < \gamma_{\text{th}}) \\
&= (\max \{\ln(1 + \gamma_{SD}) - \ln(1 + \gamma_{SE}), 0\} < \gamma_{\text{th}})^{N_t} \\
&= (Q_1)^{N_t}
\end{aligned} \tag{16}
$$

where γ_{th} is a given threshold.

Q_1 is given as

$$
\begin{aligned}
Q_1 &= \Pr(C(\gamma_{SD}, \gamma_{SE}) < \gamma_{\text{th}}) \\
&= \Pr(\gamma_{SD} < \beta\gamma_{SE} + \beta - 1) \\
&= \int_0^\infty F_{\gamma_{SD}} \ (\beta\gamma_{SE} + \beta - 1) f_{\gamma_{SE}}(\gamma_{SE}) d\gamma_{SE}
\end{aligned} \tag{17}
$$

$$= \int_0^\infty \frac{1}{\prod\limits_{d=1}^{N} \Gamma(m_d)} G_{1,3}^{2,1}\left[\frac{\beta\gamma_{SE} + \beta - 1}{\overline{\gamma_{SD}}} \prod_{d=1}^{2} \frac{m_d}{\Omega_d} \Big|_{m_1,m_2,0}^{1}\right]$$

$$\times \frac{1}{\gamma_{SE} \prod\limits_{i=1}^{N} \Gamma(m_i)} G_{0,2}^{2,0}\left[\frac{\gamma_{SE}}{\overline{\gamma_{SE}}} \prod_{i=1}^{2} \frac{m_i}{\Omega_i} \Big|_{m_1,m_2}^{-}\right] d\gamma_{SE}$$

$$\beta = \exp(\gamma_{\text{th}}) \tag{18}$$

The SOP of the suboptimal TAS scheme is given as

$$F_{\text{suboptimal}}$$
$$= \Pr(\gamma_{SDg} < \beta\gamma_{SEg} + \beta - 1)$$

$$= \Pr(\max_{1 \le i \le N_t} (\gamma_{SDi}) < \beta\gamma_{SEg} + \beta - 1)$$

$$= \int_0^\infty \left(F_{\gamma_{SD}}(\beta\gamma_{SE} + \beta - 1)\right)^{N_t} f_{\gamma_{SE}}(\gamma_{SE}) d\gamma_{SE}$$

$$= \int_0^\infty \left(\frac{1}{\prod\limits_{d=1}^{N} \Gamma(m_d)} G_{1,3}^{2,1}\left[\frac{\beta\gamma_{SE} + \beta - 1}{\overline{\gamma_{SD}}} \prod_{d=1}^{2} \frac{m_d}{\Omega_d} \Big|_{m_1,m_2,0}^{1}\right]\right)^{N_t}$$

$$\times \frac{1}{\gamma_{SE} \prod\limits_{i=1}^{N} \Gamma(m_i)} G_{0,2}^{2,0}\left[\frac{\gamma_{SE}}{\overline{\gamma_{SE}}} \prod_{i=1}^{2} \frac{m_i}{\Omega_i} \Big|_{m_1,m_2}^{-}\right] d\gamma_{SE} \tag{19}$$

Because of the complex function operation in (17), (19), there is no closed solution. In this paper, with the help of [32], the close-form expressions of the low bound on the SOP based optimal TAS scheme are derived. The low bound is given as

$$
\begin{aligned}
Q_L &= \Pr(\gamma_{SD} < \beta\gamma_{SE}) \\
&= \int_0^\infty F_{\gamma_{SD}} \ (\beta\gamma_{SE}) f_{\gamma_{SE}}(\gamma_{SE}) d\gamma_{SE} \\
&= \int_0^\infty \frac{1}{\prod\limits_{d=1}^{N} \Gamma(m_d)} G_{1,3}^{2,1}\left[\frac{\beta\gamma_{SE}}{\overline{\gamma_{SD}}} \prod_{d=1}^{2} \frac{m_d}{\Omega_d} \Big|_{m_1,m_2,0}^{1}\right] \\
&\quad \times \frac{1}{\gamma_{SE} \prod\limits_{i=1}^{N} \Gamma(m_i)} G_{0,2}^{2,0}\left[\frac{\gamma_{SE}}{\overline{\gamma_{SE}}} \prod_{i=1}^{2} \frac{m_i}{\Omega_i} \Big|_{m_1,m_2}^{-}\right] d\gamma_{SE}
\end{aligned} \tag{20}
$$

With the help of [33], we can use the method as follows, (21), as shown at the bottom of the next page, where

$$b^* = s + t - \frac{u + v}{2}$$

$$c^* = m + n - \frac{p + q}{2}$$

$$\phi = \sum_{i=1}^{p} b_i - \sum_{i=1}^{q} b_i + \frac{p - q}{2} + 1$$

$$\theta = \sum_{i=1}^{v} d_i - \sum_{i=1}^{u} c_i + \frac{u - v}{2} + 1$$

$$\Delta(k, a_n) = \frac{a_n}{k}, \frac{a_n + 1}{k}, \dots, \frac{a_n + k - 1}{k} \tag{22}$$

We can obtain

$$Q_L = \frac{1}{\prod\limits_{i=1}^{2} \Gamma(m_i) \prod\limits_{d=1}^{2} \Gamma(m_d)}$$

$$\times G_{3,3}^{3,2}\left[\frac{\overline{\gamma_{SD}} \prod\limits_{i=1}^{2} \frac{m_i}{\Omega_i}}{\beta\overline{\gamma_{SE}} \prod\limits_{d=1}^{2} \frac{m_d}{\Omega_d}} \Big|_{m_1,m_2,0}^{1-m_1,1-m_2,1}\right] \tag{23}$$

IV. THE PROBABILITY OF SPSC FOR THE OPTIMAL AND SUBOPTIMAL TAS SCHEMES

The probability of SPSC for the optimal TAS scheme is given as

$$
\begin{aligned}
F_{\text{optimal}} &= \Pr(\max_{1 \le i \le N_t}(C_i) > 0)\\
&= 1 - \Pr(\max_{1 \le i \le N_t}(C_i) < 0)\\
&= 1 - (\max\{\ln(1+\gamma_{\text{SD}}) - \ln(1+\gamma_{\text{SE}}), 0\} < 0)^{N_t}\\
&= 1 - (QQ_1)^{N_t} \quad (24)
\end{aligned}
$$

QQ_1 is given as

$$
\begin{aligned}
QQ_1 &= \Pr(C(\gamma_{\text{SD}}, \gamma_{\text{SE}}) < 0)\\
&= \Pr(\gamma_{\text{SD}} < \gamma_{\text{SE}})\\
&= \int_0^\infty F_{\gamma_{\text{SD}}}(\gamma_{\text{SE}}) f_{\gamma_{\text{SE}}}(\gamma_{\text{SE}}) d\gamma_{\text{SE}}\\
&= \int_0^\infty \frac{1}{\prod\limits_{d=1}^{N}\Gamma(m_d)} G_{1,3}^{2,1}\left[\frac{\gamma_{\text{SE}}}{\overline{\gamma}_{\text{SD}}}\prod_{d=1}^{2}\frac{m_d}{\Omega_d}\Big|_{m_1,m_2,0}^{1}\right]\\
&\quad \times \frac{1}{\gamma_{\text{SE}}\prod\limits_{i=1}^{N}\Gamma(m_i)} G_{0,2}^{2,0}\left[\frac{\gamma_{\text{SE}}}{\overline{\gamma}_{\text{SE}}}\prod_{i=1}^{2}\frac{m_i}{\Omega_i}\Big|_{m_1,m_2}^{-}\right] d\gamma_{\text{SE}}\\
&= \frac{1}{\prod\limits_{i=1}^{2}\Gamma(m_i)\prod\limits_{d=1}^{2}\Gamma(m_d)}\\
&\quad \times G_{3,3}^{3,2}\left[\frac{\overline{\gamma}_{\text{SD}}}{\overline{\gamma}_{\text{SE}}}\frac{\prod\limits_{i=1}^{2}\frac{m_i}{\Omega_i}}{\prod\limits_{d=1}^{2}\frac{m_d}{\Omega_d}}\Big|_{m_1,m_2,0}^{1-m_1,1-m_2,1}\right] \quad (25)
\end{aligned}
$$

The probability of SPSC for the suboptimal TAS scheme is given as

$$
\begin{aligned}
&F_{\text{suboptimal}}\\
&= \Pr(\gamma_{\text{SD}g} > \gamma_{\text{SE}g})\\
&= \Pr(\max_{1 \le i \le N_t}(\gamma_{\text{SD}i}) > \gamma_{\text{SE}g})\\
&= 1 - \Pr(\max_{1 \le i \le N_t}(\gamma_{\text{SD}i}) < \gamma_{\text{SE}g})\\
&= 1 - \int_0^\infty (F_{\gamma_{\text{SD}}}(\gamma_{\text{SE}}))^{N_t} f_{\gamma_{\text{SE}}}(\gamma_{\text{SE}}) d\gamma_{\text{SE}}\\
&= 1 - \int_0^\infty
\end{aligned}
$$

$$
\times\left(\frac{1}{\prod\limits_{d=1}^{N}\Gamma(m_d)} G_{1,3}^{2,1}\left[\frac{\beta\gamma_{\text{SE}}+\beta-1}{\overline{\gamma}_{\text{SD}}}\prod_{d=1}^{2}\frac{m_d}{\Omega_d}\Big|_{m_1,m_2,0}^{1}\right]\right)^{N_t}
$$

$$
\times \frac{1}{\gamma_{\text{SE}}\prod\limits_{i=1}^{N}\Gamma(m_i)} G_{0,2}^{2,0}\left[\frac{\gamma_{\text{SE}}}{\overline{\gamma}_{\text{SE}}}\prod_{i=1}^{2}\frac{m_i}{\Omega_i}\Big|_{m_1,m_2}^{-}\right] d\gamma_{\text{SE}} \quad (26)
$$

Because of the complex function operation in (26), there is no closed solution. When $N_t = 1$, the closed-form expressions of (26) is given as

$$
\begin{aligned}
F_{\text{suboptimal}} &= 1 - \frac{1}{\prod\limits_{i=1}^{2}\Gamma(m_i)\prod\limits_{d=1}^{2}\Gamma(m_d)}\\
&\quad \times G_{3,3}^{3,2}\left[\frac{\overline{\gamma}_{\text{SD}}}{\overline{\gamma}_{\text{SE}}}\frac{\prod\limits_{i=1}^{2}\frac{m_i}{\Omega_i}}{\prod\limits_{d=1}^{2}\frac{m_d}{\Omega_d}}\Big|_{m_1,m_2,0}^{1-m_1,1-m_2,1}\right] \quad (27)
\end{aligned}
$$

V. SIMULATION RESULTS

In this section, the channels are adopted as 2-Nakagami channels. $E = 1$ and $\overline{\gamma} = 10$ dB.
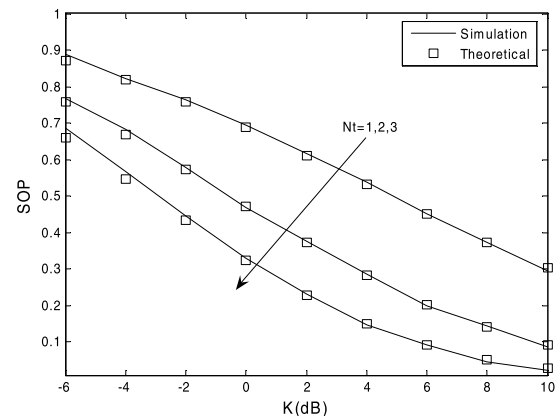
FIGURE 2. The SOP performance of the optimal TAS scheme.

In Fig. 2 and 3, the SOP performance of the two TAS schemes is presented. Table 1 shows the Monte-Carlo simulation parameters. The theoretical values are calculated in terms of (16) and (19). As shown in Fig. 2 and 3, the analytical results match the simulation results well. For fixed N_t, as

$$
\int_0^\infty x^{\alpha-1} G_{u,v}^{s,t}\left[\sigma x\Big|_{d_1,\dots,d_v}^{c_1,\dots,c_u}\right] G_{p,q}^{m,n}\left[wx^{\frac{l}{k}}\Big|_{b_1,\dots,b_q}^{a_1,\dots,a_p}\right] dx
$$

$$
= \frac{k^\phi l^{\theta+\alpha(v-u)-1}\sigma^{-\alpha}}{(2\pi)^{b^*(l-1)+c^*(k-1)}} G_{kp+lv,kq+lu}^{km+lt,kn+ls}
$$

$$
\times \left[\frac{w^k k^{k(p-q)}}{\sigma^l l^{l(u-v)}}\Big|_{\Delta(k,b_1),\dots,\Delta(k,b_m),\quad \Delta(l,1-\alpha-c_1),\dots,\Delta(l,1-\alpha-c_u),\Delta(k,b_{m+1}),\dots,\Delta(k,b_q)}^{\Delta(k,a_1),\dots,\Delta(k,a_n),\quad \Delta(l,1-\alpha-d_1),\dots,\Delta(l,1-\alpha-d_v),\Delta(k,a_{n+1}),\dots,\Delta(k,a_p)}\right] \quad (21)
$$
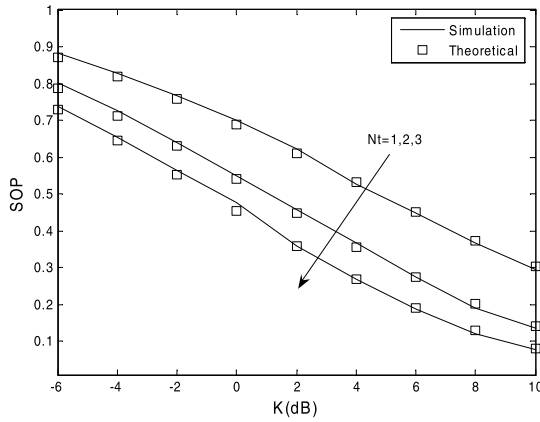
FIGURE 3. The SOP performance of the suboptimal TAS scheme.

TABLE 1. Simulation parameters.

Parameters	Values
m_{SD}	1
m_{SE}	1
V_{SD}	5 dB
V_{SE}	5 dB
N_{SD}	2
N_{SE}	2
N_t	1,2,3
γ_{th}	0 dB

the value of K is increased, the SOP performance improves. For fixed K, increasing the number of N_t improves the SOP performance.
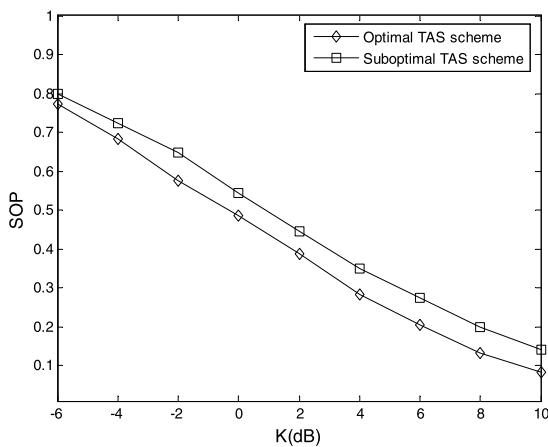

FIGURE 4. The SOP performance of the two TAS schemes.

In Fig. 4, it presents the SOP performance comparison of the two TAS schemes. Table 1 shows the simulation parameters, and $N_t = 2$. From Fig. 4, for fixed N_t, the SOP performance of optimal TAS scheme is better than that of the suboptimal TAS scheme. For example, when $K = 4dB$,

the SOP is 2.8×10^{-1} for the optimal TAS scheme, 3.6×10^{-1} for the suboptimal TAS scheme. Increasing K improves the SOP performance of the two TAS schemes. The SOP performance gap is also increased. When $K = 10dB$, the SOP is 9.2×10^{-2} for the optimal TAS scheme, 1.4×10^{-1} for the suboptimal TAS scheme.
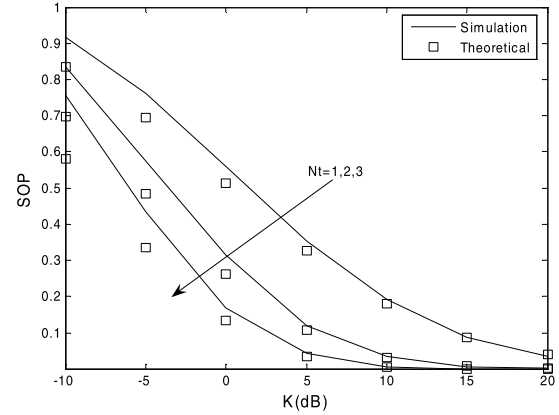

FIGURE 5. The low bound values of the SOP based the optimal TAS scheme.

Using the optimal TAS scheme, the low bound on SOP performance is analyzed in Fig. 5. The simulation parameters are shown in Table 2. We can see from Fig. 5, for fixed N_t, increasing the value of K, the Monte-Carlo simulation values are constantly approaching the theoretical values of the low bound. When K is greater than 0 dB, Monte-Carlo simulation results and the analysis results match very well, which verifies the accuracy of the previous theoretical analysis result. As shown in Fig. 2 and 3, for fixed K, increasing N_t improves the SOP performance.

TABLE 2. Simulation parameters.

Parameters	Values
m_{SD}	1
m_{SE}	1
V_{SD}	5 dB
V_{SE}	1 dB
N_{SD}	2
N_{SE}	2
N_t	1,2,3
γ_{th}	0 dB

Using the optimal TAS scheme, the low bound on SOP performance is analyzed in Fig. 5. The simulation parameters are shown in Table 2. We can see from Fig. 5, for fixed N_t, increasing the value of K, the Monte-Carlo simulation values are constantly approaching the theoretical values of the low bound. When K is greater than 0 dB, Monte-Carlo simulation results and the analysis results match very well, which verifies the accuracy of the previous theoretical analysis result.
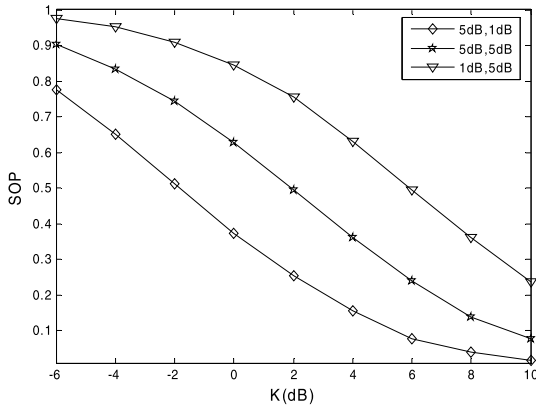
FIGURE 6. The effect of (V_{SD}, V_{SE}) on the SOP performance.

TABLE 3. Simulation parameters.

Parameters	Values	Values	Values
m_{SD}	2	2	2
m_{SE}	2	2	2
V_{SD}	5 dB	5 dB	1 dB
V_{SE}	1 dB	5 dB	5 dB
N_{SD}	2	2	2
N_{SE}	2	2	2
N_t	2	2	2
γ_{th}	0 dB	0 dB	0 dB

As shown in Fig. 2 and 3, for fixed K, increasing N_t improves the SOP performance.

Fig. 6 analyzes the effect of (V_{SD}, V_{SE}) on the SOP performance of the wireless mobile sensor communication networks. The simulation parameters are shown in Table 3. As shown in Fig. 6, for fixed value of (V_{SD}, V_{SE}), increasing the value of K can improve the SOP performance. For fixed value of K, (V_{SD}, V_{SE}) = (5dB,1dB), it can provide the best SOP performance. This is because the mobile D node is more close to the mobile S node than the mobile E node.

Fig. 7 analyzes the SOP performance of the wireless mobile sensor communication networks over 2-Rayleigh channels, 2-Nakagami channels, and Nakagami channels, respectively. The simulation parameters are shown in Table 4. As shown in Fig. 7, for fixed channels, increasing K can improve the SOP performance of the system. For fixed K, when $K < 4$dB, the SOP performance over 2-Rayleigh channels is the best; when $K > 4$dB, the SOP performance over Nakagami channels is the best. This is because when $K < 4$dB, the main channel is worse than the eavesdropping channel; when $K > 4$dB, the main channel is better than the eavesdropping channel.

Fig. 8 presents the probability of SPSC performance versus K. Table 5 gives the simulation parameters. The Monte-Carlo simulation values are constantly approaching

FIGURE 7. The effect of 2-Rayleigh, 2-Nakagami, and Nakagami channels on the SOP performance.

TABLE 4. Simulation parameters.

Parameters	2-Rayleigh	2-Nakagami	Nakagami
m_{SD}	1	2	2
m_{SE}	1	2	2
V_{SD}	5 dB	5 dB	5 dB
V_{SE}	5 dB	5 dB	5 dB
N_{SD}	2	2	1
N_{SE}	2	2	1
N_t	2	2	2
γ_{th}	0 dB	0 dB	0 dB

FIGURE 8. The probability of SPSC performance versus *K*.

the theoretical values. For fixed K, the SPSC performance is improved as m_D increases and m_E decreases. The SPSC performance for (2,1) is best. Further, it is clear that the SPSC performance improves as K increases.

Fig. 8 presents the probability of SPSC performance versus K. Table 5 gives the simulation parameters. The Monte-Carlo simulation values are constantly approaching the theoretical values. For fixed K, the SPSC performance
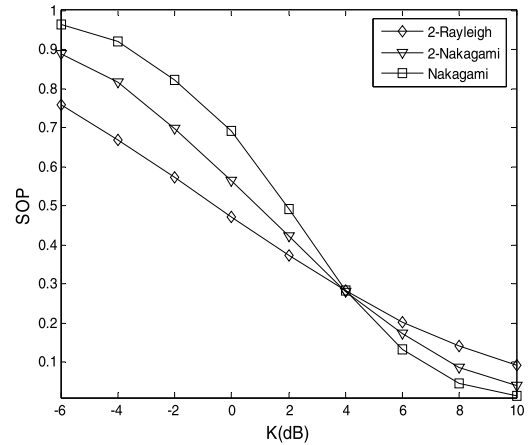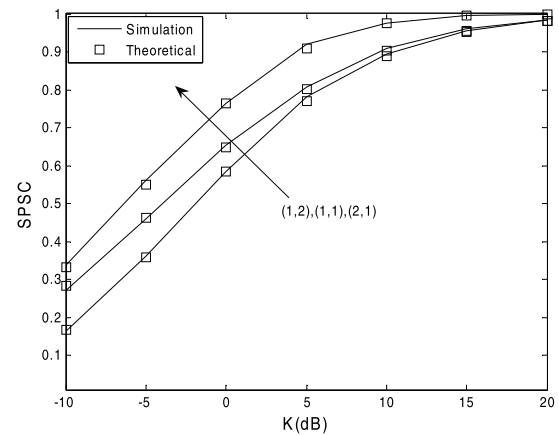
TABLE 5. Simulation parameters.

Parameters	Values	Values	Values
m_{SD}	1	1	2
m_{SE}	2	1	1
V_{SD}	5 dB	5 dB	5 dB
V_{SE}	5 dB	5 dB	5 dB
N_{SD}	2	2	2
N_{SE}	2	2	2

is improved as m_D increases and m_E decreases. The SPSC performance for $(2,1)$ is best. Further, it is clear that the SPSC performance improves as K increases.

VI. CONCLUSIONS

In this paper, the secrecy performance of the wireless mobile sensor communication networks over 2-Nakagami fading channels was investigated. We used Wyner's wiretap model, and derived the exact closed-form SOP and probability of SPSC expressions for two TAS schemes. The exact closed-form expressions for the lower bound on the SOP for optimal TAS scheme were also derived. We used Monte-Carlo simulations to verify and analyze the secrecy performance of the wireless mobile sensor communication networks. In order to improve the SOP performance, the transmit antenna N_t or relative position gain (V_{SD}, V_{SE}) should be optimized. This paper research was based on the condition that the channel was independent. But in real environment, the channel was not completely independent. In our future research, we could further study the influence of related channels on the SOP performance.

REFERENCES

[1] H. Kim, L. Mokdad, and J. Ben-Othman, "Designing UAV surveillance frameworks for smart city and extensive ocean with differential perspectives," *IEEE Commun. Mag*, vol. 56, no. 4, pp. 98–104, Apr. 2018.

[2] M. Mohammadi and A. Al-Fuqaha, "Enabling cognitive smart cities using big data and machine learning: Approaches and challenges," *IEEE Commun. Mag.*, vol. 56, no. 2, pp. 94–101, Feb. 2018.

[3] C. Kai, H. Li, L. Xu, Y. Li, and T. Jiang, "Energy-efficient device-to-device communications for green smart cities," *IEEE Trans. Ind. Informat.*, vol. 14, no. 4, pp. 1542–1551, Apr. 2018.

[4] N.-S. Vo, T. Q. Duong, M. Guizani, and A. Kortun, "5G optimized caching and downlink resource sharing for smart cities," *IEEE Access*, vol. 6, pp. 31457–31468, May 2018.

[5] L. Wan, X. Kong, and F. Xia, "Joint range-Doppler-angle estimation for intelligent tracking of moving aerial targets," *IEEE Internet Things J.*, vol. 5, no. 3, pp. 1625–1636, Jun. 2018.

[6] H. Wang, W. Du, and L. Xu, "A new sparse adaptive channel estimation method based on compressive sensing for FBMC/OQAM transmission network," *Sensors*, vol. 16, no. 7, p. 966, Jul. 2016.

[7] L. Wan, G. Han, H. Wang, L. Shu, N. Feng, and B. Peng, "Wearable sensor localization considering mixed distributed sources in health monitoring systems," *Sensors*, vol. 16, no. 3, p. 368, Mar. 2016.

[8] L. Wan, G. Han, D. Zhang, A. Li, and N. Feng, "Distributed DOA estimation for arbitrary topology structure of mobile wireless sensor network using cognitive radio," *Wireless Pers. Commun.*, vol. 93, no. 2, pp. 431–445, Feb. 2017.

[9] L. Cui, G. Xie, Y. Qu, L. Gao, and Y. Yang, "Security and privacy in smart cities: Challenges and opportunities," *IEEE Access*, vol. 6, pp. 46134–46145, Jul. 2018.

[10] K. Zhang, J. Ni, K. Yang, X. Liang, J. Ren, and X. S. Shen, "Security and privacy in smart city applications: Challenges and solutions," *IEEE Commun. Mag.*, vol. 55, no. 1, pp. 122–129, Jan. 2017.

[11] L. Sun and Q. H. Du, "Physical layer security with its applications in 5G networks: A review," *China Commun.*, vol. 14, no. 12, pp. 1–14, Dec. 2017.

[12] M. I. Zahurul and T. Ratnarajah, "Secrecy capacity and secure outage performance for Rayleigh fading SIMO channel," in *Proc. ICASSP*, Prague, Czech Republic, May 2011, pp. 1900–1903.

[13] H. Alves, R. D. Souza, and M. Debbah, "Enhanced physical layer security through transmit antenna selection," in *Proc. GLOBECOM*, Houston, TX, USA, Dec. 2011, pp. 879–883.

[14] H. Alves, R. D. Souza, M. Debbah, and M. Bennis, "Performance of transmit antenna selection physical layer security schemes," *IEEE Signal Process. Lett.*, vol. 19, no. 6, pp. 372–375, Jun. 2012.

[15] N. Yang, P. L. Yeoh, M. Elkashlan, R. Schober, and I. B. Collings, "Transmit antenna selection for security enhancement in MIMO wiretap channels," *IEEE Trans. Commun.*, vol. 61, no. 1, pp. 144–154, Jan. 2013.

[16] N. Li, X. Tao, and J. Xu, "Ergodic secrecy sum-rate for downlink multiuser MIMO systems with limited CSI feedback," *IEEE Commun. Lett.*, vol. 18, no. 6, pp. 969–972, Jun. 2014.

[17] Y. Cao *et al.*, "Optimization or alignment: Secure primary transmission assisted by secondary networks," *IEEE J. Sel. Areas Commun.*, vol. 36, no. 4, pp. 905–917, Apr. 2018.

[18] S. Althunibat, V. Sucasas, and J. Rodriguez, "A physical-layer security scheme by phase-based adaptive modulation," *IEEE Trans. Veh. Technol.*, vol. 66, no. 11, pp. 9931–9942, Nov. 2017.

[19] S. Althunibat, A. Antonopoulos, E. Kartsakli, F. Granelli, and C. Verikoukis, "Countering intelligent-dependent malicious nodes in target detection wireless sensor networks," *IEEE Sensors J.*, vol. 16, no. 23, pp. 8627–8639, Dec. 2016.

[20] X. Wang, M. Huang, X. Wu, and G. Bi, "Direction of arrival estimation for MIMO radar via unitary nuclear norm minimization," *Sensors*, vol. 17, no. 4, p. 939, Apr. 2017.

[21] X. Wang, L. Wang, X. Li, and G. Bi, "Nuclear norm minimization framework for DOA estimation in MIMO radar," *Signal Process.*, vol. 135, pp. 147–152, Jun. 2017.

[22] S. Althunibat, V. Sucasas, G. Mantas, and J. Rodriguez, "Physical-layer entity authentication scheme for mobile MIMO systems," *IET Commun.*, vol. 12, no. 6, pp. 712–718, Jun. 2018.

[23] L. W. Xu *et al.*, "Physical layer security performance of mobile vehicular networks," *Mobile Netw. Appl.*, to be published.

[24] G. K. Karagiannidis, N. C. Sagias, and P. T. Mathiopoulos, "*N*-Nakagami: A novel stochastic model for cascaded fading channels," *IEEE Trans. Commun.*, vol. 55, no. 8, pp. 1453–1458, Aug. 2007.

[25] S. Q. Nguyen and H. Y. Kong, "Outage probability analysis in dual-hop vehicular networks with the assistance of multiple access points and vehicle nodes," *Wireless Pers. Commun.*, vol. 87, no. 4, pp. 1175–1190, Apr. 2016.

[26] S. Ö. Ata and I. Altunbaş, "STTC design for vehicular communication systems employing fixed-gain AF PLNC over cascaded fading channels," *IET Commun.*, vol. 12, no. 11, pp. 1283–1289, Nov. 2018.

[27] L. Xu, J. Wang, H. Zhang, and T. A. Gulliver, "Performance analysis of IAF relaying mobile D2D cooperative networks," *J. Franklin Inst.*, vol. 354, no. 2, pp. 902–916, Jan. 2017.

[28] L. Xu, J. Wang, Y. Liu, W. Shi, and T. A. Gulliver, "Outage performance for IDF relaying mobile cooperative networks," *Mobile Netw. Appl.*, vol. 23, no. 6, pp. 1496–1501, Dec. 2018.

[29] L. Xu, H. Zhang, J. Wang, and T. A. Gulliver, "Joint TAS/SC and power allocation for IAF relaying D2D cooperative networks," *Wireless Netw.*, vol. 23, no. 7, pp. 2135–2143, Jul. 2017.

[30] M. Bloch, J. Barros, M. R. D. Rodrigues, and S. W. McLaughlin, "Wireless information-theoretic security," *IEEE Trans. Inf. Theory*, vol. 54, no. 6, pp. 2515–2534, Jun. 2008.

[31] H. Le *et al.*, "Performance analysis of physical layer security over generalized-*K* fading channels using a mixture gamma distribution," *IEEE Commun. Lett.*, vol. 20, no. 2, pp. 408–411, Feb. 2016.

[32] V. S. Adamchik and O. I. Marichev, "The algorithm for calculating integrals of hypergeometric type functions and its realization in REDUCE system," in *Proc. SAC*, Tokyo, Japan, 1990, pp. 212–224.

HAN WANG received the B.S. degree in electrical engineering from the Hubei University of Nationalities, China, in 2009, and the M.S. and Ph.D. degrees in information and communication system from Hainan University, Haikou, China, in 2013 and 2017, respectively. He was with China Mobile, Jiangxi branch, as a Network Engineer for one year. He is currently an Associate Professor with Yichun University. His research interests include wireless sensor networks, filter-bank multicarrier communications, and information theory.

PINGPING XIAO received the B.S. and M.S. degrees in optical engineering from Jiangxi Normal University, China, in 2003 and 2006, respectively, and the Ph.D. degree from Shanghai Jiaotong University, China, in 2012. He is currently a Professor with Yichun University. His current research interests include optical communications and optical sensor applications.

LINGWEI XU was born in Shandong, China, in 1987. He received the M.E. degree in electronics and communication engineering and the Ph.D. degree from the Ocean University of China, China, in 2013 and 2016, respectively. He is currently an Associate Professor with the Qingdao University of Science and Technology. His research interests include wireless sensor networks, MIMO wireless systems, and M2M wireless communications.

WENZHONG LIN was born in Fujian, China, in 1965. He received the M.E. degree in electrical engineering from Fuzhou University, China, in 1990, and the Ph.D. degree from Nagasaki University, Japan, in 2016. He is currently a Professor with Minjiang University. His research interests include the Internet of Things, computer control technology, and servo drive technology.

RUHONG WEN received the B.S. degree in physics from Jiangxi Normal University, in 2001, and the master's degree in optical engineering from China Jiliang University, in 2007. Since 2007, she has been with the College of Physical Science and Technology, Yichun University, where she has been an Associate Professor, since 2013. She has published over 20 papers. Her research interests include image encryption and information theory.

• • •